CHIN. PHYS. LETT. Vol. 26, No. 6 (2009) 068501

Two Possible Configurations for Silver–C_{60}–Silver Molecular Devices and Their Conductance Characteristics *

TIAN Guang-Jun(田广军), SU Wen-Yong(苏文勇)**

Department of Physics, Beijing Institute of Technology, Beijing 100081
Department of Theoretical Chemistry, Royal Institute of Technology, AlbaNova S-10691, Stockholm, Sweden

(Received 9 December 2008)

Coherent electronic transport properties of silver–C_{60}–silver molecular junctions in different configurations are studied using hybrid density function theory. The experimentally measured current flows of C_{60} molecules adsorbed on the silver surface are well reproduced by theoretical calculations. It is found that the current–voltage characteristics of the molecular junctions depend strongly on the configurations of the junctions. Transmission spectra combined with density of states can help us to understand in depth the transport properties. Different kinds of electrode construction are also discussed. With the help of the calculation, two possible configurations of silver–C_{60}–silver molecular junctions are suggested.

PACS: *85.65.+h, 73.63.−b*

Great efforts have been made to study the adsorption of C_{60} molecules on metal surface in the past several years.[1−5] In studies of C_{60}–metal interactions, low-dimensional ordered C_{60}-based films, especially C_{60} on Ag(100), have attracted particular attention.[2,5,6] So far, a number of fascinating properties of C_{60}/Ag(100) have been reported, such as strong C_{60} charge transfer[7] and the opening of an energy gap when the temperature is below 250 K.[8] Most of the previous studies of C_{60}/Ag(100) have been focused on its unusual geometric structure. However, the basic configurations of C_{60} molecules when they are adsorbed on an Ag(100) surface are still unclear, such as the origin of the bright–dim (BD) contrast observed in scanning tunneling microscopy (STM) images.[2,5,9−11] Furthermore, fewer studies have investigated the current–voltage (I–V) characteristics of C_{60}/Ag(100). The I–V characteristics of an electronic circuit in which molecular systems act as conducting elements is one of the major themes in molecular electronics.[12] It can give important information for the potential applications of devices based on molecular systems.

Different C_{60} geometric organizations and different molecular orientations have been utilized to analyze the BD contrast and it has been confirmed that the major BD contrast comes from different geometric effects, and purely different molecular orientations do not induce large enough differences in the electronic states to explain the experimental findings. Recently, Zhang *et al.*[6] have studied the geometric and electronic structure of a C_{60} monolayer on Ag(100) by using scanning tunneling microscopy and spectroscopy. The measured I–V spectra of different positions on the monolayer fell into different groups, indicating that there are different kinds of electronic structures in the C_{60} monolayer[6] in C_{60}/Ag(100). These findings are very interesting. In this Letter, we focus our attention on local contact. We suggest two geometry configurations from the symmetry, and use first principles calculations within the framework of the density functional theory[13−15] to investigate the coherent electronic transport properties of silver–C_{60}–silver molecular junctions. Through the simulation, we find that there are two types of contacts which are possible configurations for silver–C_{60}–silver molecular devices. We also analyze the relations between our results and those of Zhang *et al.*[6]

Our theoretical framework was originally proposed a few years ago,[14,16−18] and was an extension of the scattering theory approaches developed by the groups of Mujica *et al.*,[19] Samanta *et al.*[20] and Tian *et al.*[21] In our approach, we divide the molecular device into three parts: source, drain and extended molecule. The source and drain are described by an effective mass approximation (EMA), while the extended molecule is treated with hybrid density functional theory. Therefore, our approach combines the advantage of solid state methods that can accurately describe the bulk electrode, and the advantage of quantum chemistry which can characterize precisely the extended molecule part. In the equilibrium state, the extended molecule is in equilibrium with the source and the drain through the line up of their effective Fermi levels. Because the molecule is only a small perturbation to the electrodes, the Fermi level of the whole molecular device at equilibrium should be the Fermi level of the electrodes. A good question to ask is where E_f lies relative to the molecular energy levels. A convenient method is to set the middle of the

*Supported by the Scientific Research Foundation for Returned Overseas Chinese Scholars of Ministry of Education of China under Grant No 20070732022.

**To whom correspondence should be addressed. Email: suwy@bit.edu.cn

© 2009 Chinese Physical Society and IOP Publishing Ltd

highest occupied molecular orbital (HOMO) and the lowest unoccupied molecular orbital (LUMO) of the finite system at the position of the electrodes' Fermi level, and move the molecular energy levels up or down rigidly relative to the electrodes' Fermi level. Then we can utilize the advantage of bulk electrode parameters and overcome the shortcoming of finite models. In the absence of an experimental setup, by treating the position of E_f as an adjustable parameter we can take into account the effect of charge transfer.[22] In a nonequilibrium state, we assume that the drain is grounded, the potential energy of the source is lifted by the external bias of V_D.[17]

In the one-dimensional situation, the current density through the molecular junction can be written as[18,23]

$$i_{1D} = \frac{2\pi e}{\hbar}\int_{eV_D}^{\infty}[f(E-eV)-f(E)]|T(E,V)|^2 \cdot n^S(E)n^D(E)dE, \quad (1)$$

where $n^S(E)$ and $n^D(E)$ are the density of states (DOS) of the source and drain respectively, and $f(E)$ is the Fermi distribution function. Then the current through the molecular junctions can be computed by the relationship $I_{1D} = i_{1D}$.

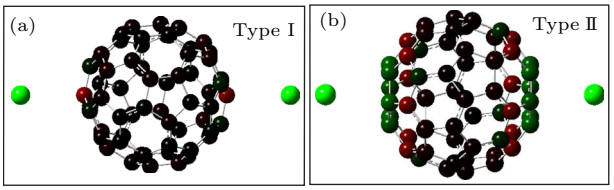

Fig. 1. (Color online) Structures and charge distributions of (a) a type-I molecular junction and (b) a type-Ⅱ molecular junction. These two types of junctions are used to describe two different kinds of configurations of silver–C_{60}–silver molecular devices. Here green denotes positive charge and red denotes negative charge.

In our simulation, we adopt two models (named as type-I and type-Ⅱ) to describe the silver–C_{60}–silver molecular device(shown in Fig. 1). In type-I, as shown in Fig. 1(a), both Ag atoms are deposited on the same line with two symmetrical carbon atoms. The C_{60} molecule is attached to the Ag electrodes with a 3.20 Å carbon-electrode distance at each side. In type-Ⅱ, as shown in Fig. 1(b), both Ag atoms are deposited on the extended line which connects the centers of the two opposite hexagon faces on the C_{60} molecule with a distance of 3.00 Å from Ag atoms to hexagon face. The lengths of type-I and type-Ⅱ are 13.55 Å and 12.55 Å respectively. Type-I is 1.0 Å longer than type-Ⅱ.

The geometrical optimizations and the electronic structure calculations are carried out at hybrid density functional theory (DFT) B3LYP level with the LANL2DZ basis set using the Gaussian-03 package.[24] The coherent electronic transport properties of the silver–C_{60}–silver molecular junctions are calculated using the Quantum Chemistry for Molecular Electronics (QCME) program.[25] The QCME program has been applied to different molecular junctions for both elastic and inelastic scattering processes. The calculated results are in good agreement with the experiments.[14,15]

Table 1. Summary of the orbital energies of HOMO, LUMO and the total energies (in eV) of the single molecule, type-I molecular junction and the type-Ⅱ molecular junction, computed at the B3LYP level.

	Single C_{60} molecule	Type-I molecular junction	Type-Ⅱ molecular junction
HOMO	−6.72	−4.63	−4.54
LUMO	−3.89	−4.33	−4.17
Total energy	−62197.69	−70129.74	−70129.59

The energies of the HOMOs, LUMOs and total energies of the two extended molecules are listed in Table 1. The increase of the energies of the HOMOs and the decrease of the energies of the LUMOs, compared with single molecule, result in smaller energy gaps, so the conduction ability of the molecular junctions will increase. The middle values of the HOMOs and LUMOs are −4.48 eV and −4.35 eV, respectively, close to the Fermi level of bulk Ag (−4.3 eV), so the molecular energy levels do not need to be adjusted greatly. The total energies of extended molecular junctions are lower than single molecule, and the total energy of a type-I molecular junction is lower than that of a type-Ⅱ molecular junction. This means that the stability of type-I is higher than type-Ⅱ.

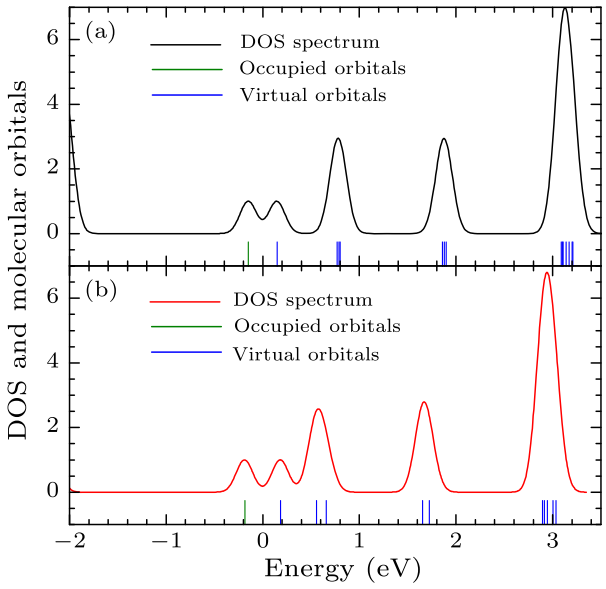

Fig. 2. (Color online) The density of states and the molecular orbits of the model molecular junction for (a) type-I and (b) type-Ⅱ. We set the E_f as the origin of energy.

Figure 1 shows the distribution of charge in both molecular junctions. Green denotes positive charge and red denotes negative charge. For both junctions, the silver electrodes exhibit positive electrical characteristics, and the C_{60} molecules exhibit negative elec-

trical characteristics. This means that the free electrons transfer from the electrodes to the molecules. In the type-I molecular junction, the terminal carbon atoms are negative. The interactions between electrodes and molecule are attraction and beneficial to conductance. However, in the type-Ⅱ molecular junction, the terminal carbon atoms are positive, so the interactions between electrodes and molecule are not helpful to conductance. We also find that the electrons transfer $0.25e$ per C_{60} molecule, which is similar to the result ($0.15e$) reported by Lu *et al.* for an isolated C_{60} molecule on Ag(100).[26] Because the quantity is small, this will not affect the current–voltage greatly.

To investigate the electronic structures thoroughly, we have calculated the density of states (DOS) and the corresponding molecular orbits of both molecular junctions, as shown in Fig. 2. For both types of molecular junctions, there are five peaks in the DOS curves. The first two peaks correspond to the highest occupied molecular orbit (HOMO) and the lowest unoccupied molecular orbit (LUMO), respectively. The corresponding orbits of the last three DOS peaks are the higher unoccupied molecular orbits (starting from the LUMO+1). We compare the orbital electron densities of the LUMO with LUMO+1 (Fig. 3). The electron densities of the two LUMOs concentrate on one side of the molecular junctions, whereas a dispersive distribution is found in the LUMO+1s. Since one basic reason for the appearance of conductance channels is the strong connections between the electrodes and the molecule, a dispersive distribution of the orbital electron is helpful in this connection and vice versa. Thus we can deduce that, for both model molecular junctions, the first conduction channels appear from the LUMO+1s, and the LUMOs do not contribute to the conductance channels.

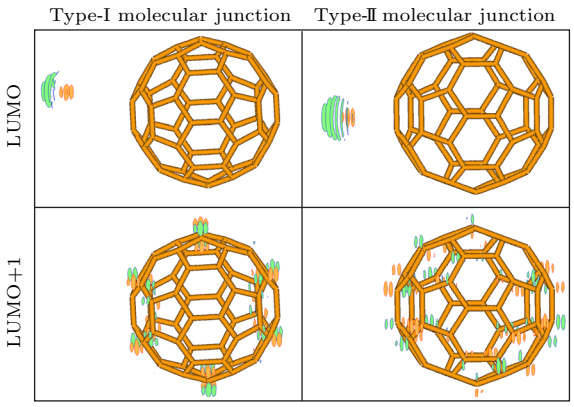

Fig. 3. (Color online) The distribution of the orbital electrons of the LUMO and LUMO+1 of the extended molecule.

To understand the transport character quantitatively, we give the transmission spectra (as a function of orbital energies) for both molecular junctions, as illustrated in Fig. 4. When the bias voltage is in the range from 0 V to 2 V, the current depends mostly on the transmission ranging from 0 eV to 2 eV. The peaks on the transmission spectra indicate the possible conduction bands of the molecular junctions. Conduction bands are transport channels for the electrons. When the sample bias increases, the energies of the injection electrons increase as well. Once the energies of the injection electrons are higher than the minimum energy of the conduction band, the electrons will tunnel through the band easily and the tunnel current will increase sharply. Before the energies of the injection electrons arrive at the minimum energy of the next conduction band, the current will be a nearly stable value. This explains that when accompanied by the increase of bias voltage, obvious steps will appear on the I–V curves as a result of increasing energy of the injection electrons. The transmission spectra seem to indicate that there are still conduction bands between 2.5 eV and 3.5 eV. We calculate the transmission considering the field at $V_{sd} = 1$ V, the transmission does not show great change.

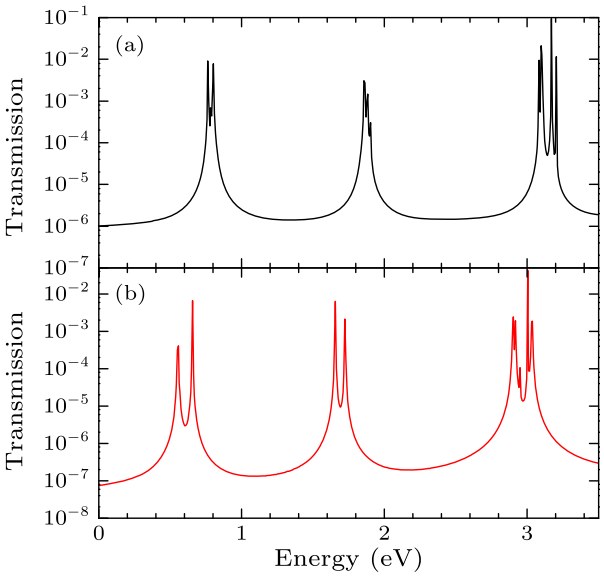

Fig. 4. (Color online) Transmission spectra of type-I (a) and type-Ⅱ (b) molecular junctions, respectively. Here we set the Fermi energy level as 0.

Comparing the DOS curves with the transmission spectra, we find that the last three DOS peaks for both molecular junctions correspond one-to-one with the peaks in the transmission spectra. However, there are not any relevant peaks appearing in the transmission curves corresponding to the first two peaks. This means that the HOMO and LUMO do not contribute to the conduction bands here. Because we do not consider the conduction of the hole here, the HOMO does not contribute to the conductance channels. The LUMO's transmission is consistent with the foregoing analysis of its electron density distribution (see Fig. 3). Therefore, there are neither any peaks in the

transmission spectra nor any steps in the I–V curves corresponding to the LUMOs.

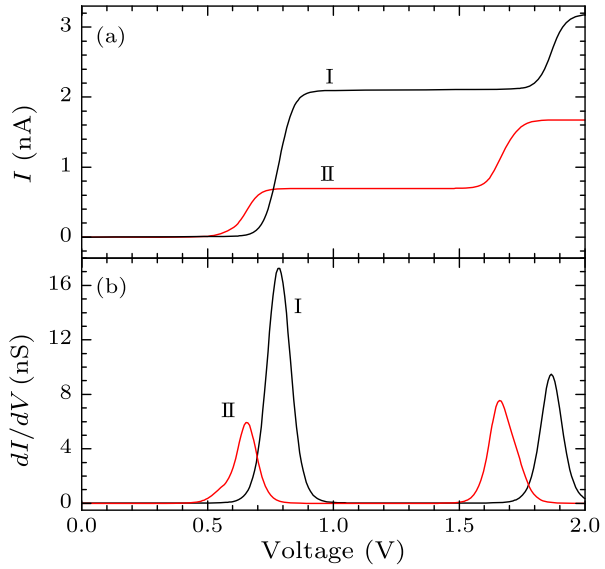

Fig. 5. (Color online) Calculated result for the current (a) and conductance (b) characteristics of type-I (Black line) and type-Ⅱ (Red line) molecular junctions.

Figure 5 illustrates our calculated results for the current and the conductance as a function of bias voltage for two configurations. The I–V curves of type-I and type-Ⅱ molecular junctions (as shown in Fig. 5(a)) can be distinguished effortlessly. The current of type-I is always larger than that of type-Ⅱ. At a voltage of 2.0 V, the currents of type-I and type-Ⅱ are 3.0 nA and 1.5 nA respectively. Comparing our calculation results with the experimental curves,[6] we find that the I–V curves for type-I molecular junctions and bright (B) molecules, type-Ⅱ molecular junctions and dim molecules(DM) are in good agreement. Thus we think that these two configurations are two possible structures when C_{60} molecules are adsorbed on a silver surface. We are aware of the experiment in Ref. [2], it was found that 99% of all bright molecules are oriented with a 5–6 bond (the bond between a pentagon and a hexagon) facing up, while 84% of all dim molecules are oriented with a 6–6 bond (the bond between two hexagons) facing up. Comparing our calculations with the simulations from Zhang and coworkers[6] and analyzing the geometry structures, we think the type-I geometry structure is close to 5–6 bond facing up, and the type-Ⅱ geometry structure is close to 6–6 bond facing up. If we denote the two carbon atoms in the 5–6 bond as 1 and 2, and their centrosymmetric carbon atoms as 3 and 4, we can construct type-I configuration extended molecules through 1-3 and 2-4. Similarly, through two neighbor hexagon centers and their centrosymmetric positions we can construct type-Ⅱ configuration extended molecules. However, these need further calculations.

In conclusion, we have studied the coherent electronic transport properties of molecular junctions consisting of C_{60} molecules and silver surfaces using a hybrid density-function theory. The current–voltage characteristics of our calculations are in good agreement with experimental results.

References

[1] Harneit W, Boehme C, Schaefer S, Huebener K, Fostiropoulos K and Lips K 2007 *Phys. Rev. Lett.* **98** 216601
[2] Grobis M, Lu X and Crommie M F 2002 *Phys. Rev.* B **66** 161408
[3] Wang L L and Cheng H P 2004 *Phys. Rev.* B **69** 165417
[4] Menech M D, Saalmann U and Garcia M E 2006 *Phys. Rev.* B **73** 155407
[5] Pai W W and Hsu C L 2003 *Phys. Rev.* B **68** 121403(R)
[6] Zhang X Q, He W, Zhao A D, Li H N, Chen L, Pai W W, Hou J G, Loy M M T, Yang J L and Xiao X D 2007 *Phys. Rev.* B **75** 235444
[7] Cepek C, Sancrotti M, Greber T and Osterwalder J 2000 *Surf. Sci.* **454** 467
[8] Cepek C, Vobornik I, Goldoni A, Magnano E, Selvaggi G, Kröger J, Panaccione G, Rossi G and Sancrotti M 2001 *Phys. Rev. Lett.* **86** 3100
[9] Cepek C, Fasel R, Sancrotti M, Greber T and Osterwalder J 2001 *Phys. Rev.* B **63** 125406
[10] Hsu C L and Pai W W 2003 *Phys. Rev.* B **68** 245414
[11] Brouet V, Yang W L, Zhou X J, Choi H J, Louie S G, Cohen M L, Goldoni A, Parmigiani F, Hussain Z and Shen Z X 2004 *Phys. Rev. Lett.* **93** 197601
Brouet V, Yang W L, Zhou X J, Choi H J, Louie S G, Cohen M L, Goldoni A, Parmigiani F, Hussain Z and Shen Z X 2005 *Phys. Rev. Lett.* **95** 099903
[12] Nitzan A and Ratner M A 2003 *Science* **300** 1384
[13] Hohenberg P and Kohn W 1964 *Phys. Rev.* **136** B864
[14] Su W Y, Jiang J and Luo Y 2005 *Chem. Phys. Lett.* **412** 406
[15] Su W Y, Jiang J, Lu W and Luo Y 2006 *Nano Lett.* **6** 2091
[16] Wang C K, Fu Y and Luo Y 2001 *Phys. Chem. Chem. Phys.* **3** 5017
[17] Luo Y, Wang C K and Fu Y 2002 *J. Chem. Phys.* **117** 10283
[18] Wang C K and Luo Y 2003 *J. Chem. Phys.* **119** 4923
[19] Mujica V, Kemp M, Ratner M A 1994 *J. Chem. Phys.* **101** 6849
[20] Samanta M P, Tian W, Datta S, Henderson J I, Kubiak C P 1996 *Phys. Rev.* B **53** R7626
[21] Tian W, Datta S, Hong S, Henderson J I, Kubiak C P 1998 *J. Chem. Phys.* **109** 2874
[22] Zahid F, Ghosh A W, Paulsson M, Polizzi E and Datta S 2004 *Phys. Rev.* B **70** 245317
[23] Jiang J, Lu W and Luo Y 2004 *Chem. Phys. Lett.* **400** 336
[24] Frisch M J et al 2003 $G_{AUSSIAN}03$, Revision A.1. (Pittsburgh, PA: Gaussian)
[25] Jiang J and Luo Y $Q_{CME}-V1.0$ (Quantum Chemistry for Molecular Electronics) (Sweden: Royal Institute of Technology)
[26] Lu X H, Grobis M, Khoo K H, Louie S G and Crommie M F 2004 *Phys. Rev.* B **70** 115418